SUPPORTING INFORMATION

Quantitative aspects of the interfacial catalytic oxidation of Dithiothreitol (DTT) by dissolved oxygen in the presence of carbon nanoparticles.

Jean-Jacques Sauvain[1]*, *Michel J. Rossi*[2]

[1] Institute for Work and Health, University of Lausanne and Geneva, Route de la Corniche 2, CH-1066 Epalinges-Lausanne, Switzerland

[2] Paul Scherrer Institute, Laboratory of Atmospheric Chemistry (LAC), CH-5232 Villigen PSI, Switzerland

* : Corresponding author.

e-mail address : jean-jacques.sauvain@hospvd.ch Phone : +41 21 314 74 34

Number of pages : 11

Number of figures : 5

Number of tables : 3

O_2 consumption assay

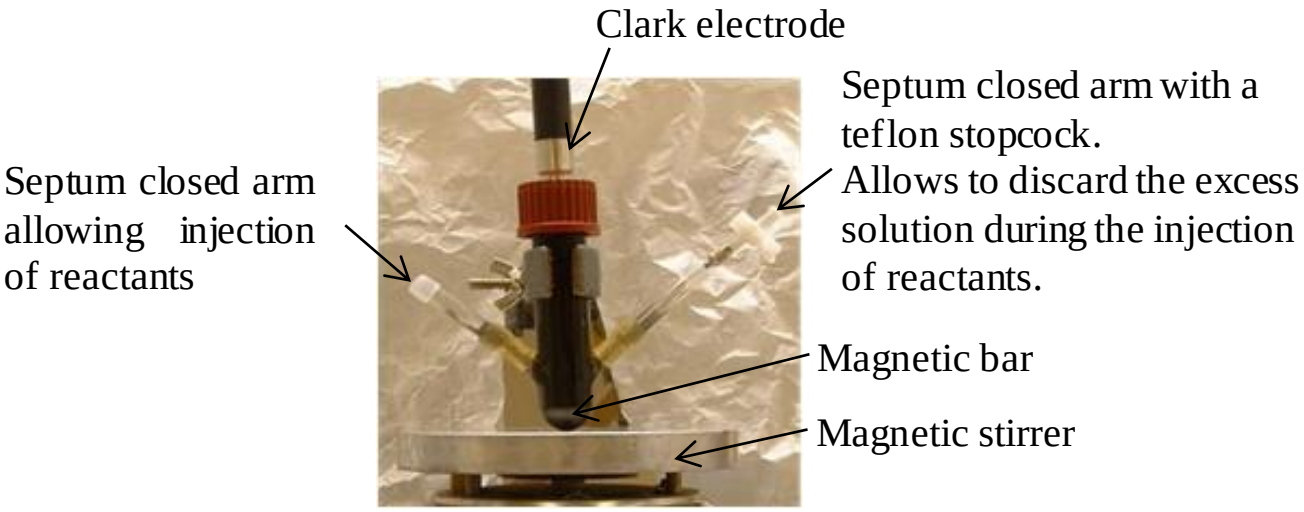

Figure S1: Picture of the reactor used for the oxymetry.

Table S1: Experimental DTT and O_2 consumption rate, bulk chemical composition (organic carbon – OC, and elemental carbon – EC) and amount of some surface functions for the studied carbonaceous nanoparticles.

	FW2	Printex 90	SRM 2975
DTT [pmol min^{-1} μg^{-1}]	124±29	67±18	41±5
Initial O_2 decay rate [μM min^{-1}]	6.1±2.5	2.8±2.4	1.8±0.7
Bulk composition:			
OC [mg g^{-1}]	60±8	17±6	55±6
EC [mg g^{-1}]	716±12	894±22	740±89
Surface functions:			
BET [m^2 g^{-1}]	460	254	91
Acidic sites [mg^{-1}] (N_{TMA})	2.4±0.2E+17	7.7±0.7E+15	4.9±0.5E+16
Carbonyl sites [mg^{-1}] (N_{NH2OH})	4.4±0.4E+17	3.1±0.3E+16	1.3±0.1E+18
Sum of all reducing sites [mg^{-1}] (N_{O3})	4.6±0.4E+17	4.3±0.5E+17	8.3±0.7E+15
Strongly reducing sites [mg^{-1}] (N_{NO2})	4.4±0.3E+16	2.8±0.2E+16	3.2±0.3E+15

BET: Brunnauer-Emmett-Teller specific surface area

TMA: Trimethylamine probe gas

NH_2OH: Hydroxylamine probe gas

O_3: Ozone probe gas

NO_2: Nitrogen dioxide probe gas

Dependence of the initial rate of DTT consumption as a function of the initial DTT concentration

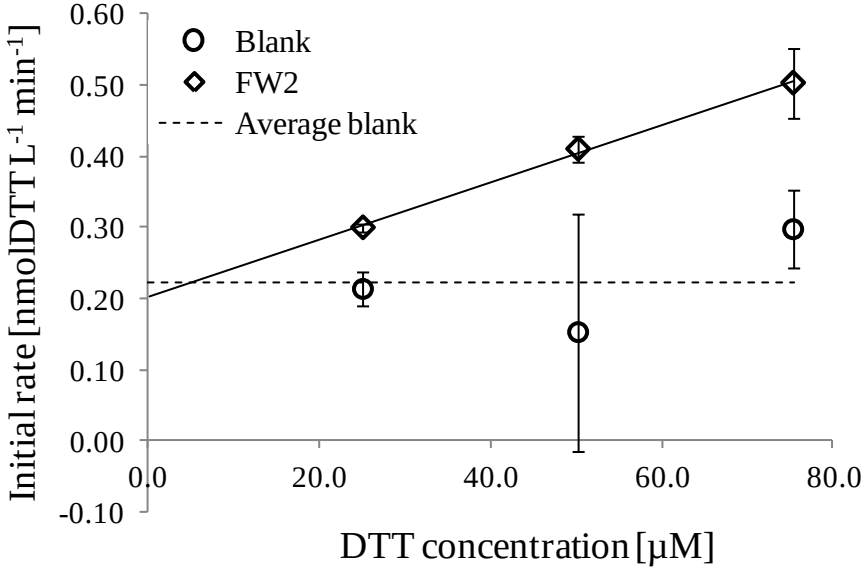

Figure S2: Dependence of the initial rate of DTT consumption as a function of the initial DTT concentration for suspended FW2 NP's. Conditions: Volume: 10 ml, FW2: 1.4 µg/ml.

Correlation of the mass-based DTT reactivity with strongly reducing surface functional groups

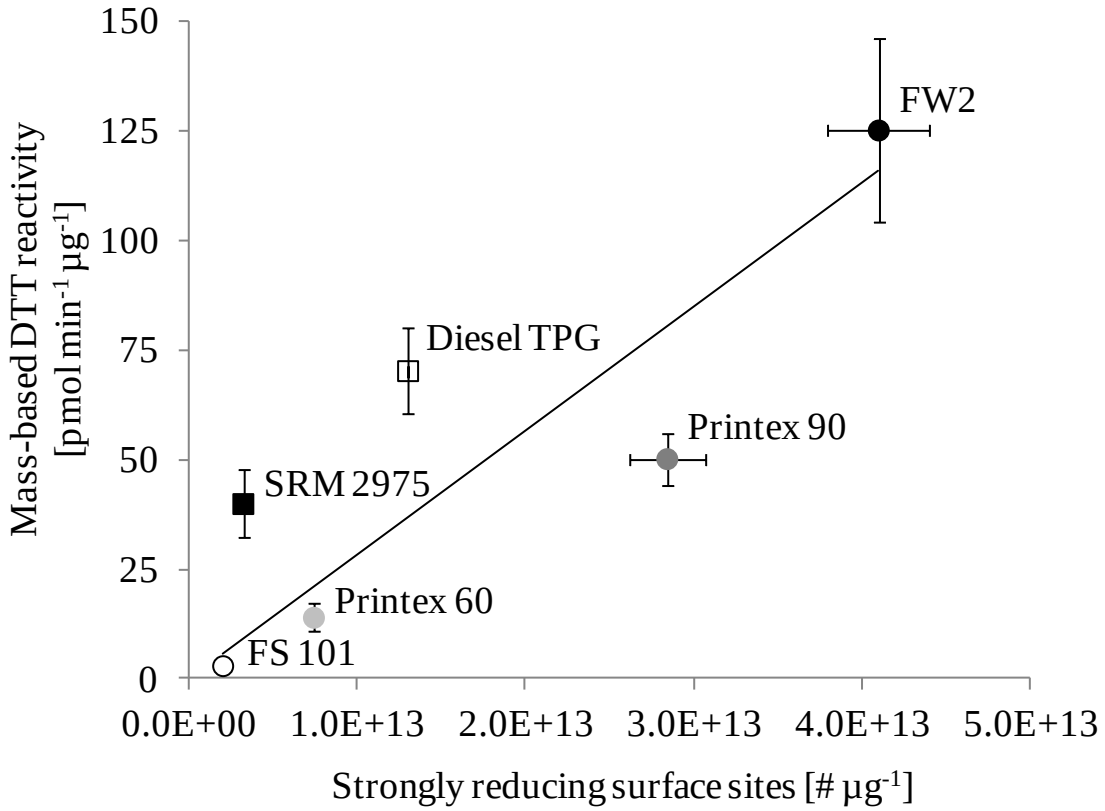

Figure S3: Correlation of the mass-based DTT reactivity of different carbonaceous nanoparticles in aqueous solution at ambient temperature against the number of strongly reducing surface functional groups per mg obtained using NO_2 as a probe gas in the heterogeneous surface titration.[1] FW2, Printex 90, Printex 60 and FS 101 are carbon black particles, whereas SRM 2975 and Diesel TPG originate from diesel engines.

Rate Law for O_2 disappearance in the presence of carbonaceous NP substrates

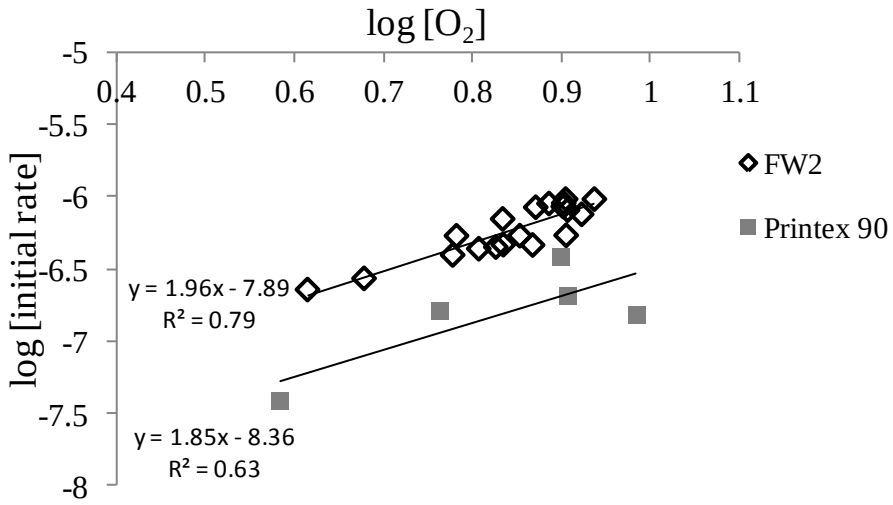

Figure S4: Order plot for O_2-dependence of initial rate of O_2 consumption (oxymetry) : representation of the log [Initial Rate] vs. log O_2 concentration. The slope of the linear regression is 1.96 for FW2 and 1.85 for Printex. Total spread of FW2 data (min-max) regarding the initial rate is less than a factor of two (standard deviation is smaller), a factor of three for the dependence on O_2 concentration.

The rate law order is consistent with a quadratic dependence of $[O_2]$ on the initial rate of oxygen consumption (see Table S2) as the averaged value $((7.84\pm0.92).10^{-3}$, coefficient of variation of 12%) presents a lower coefficient of variation compared to the linear dependence of $[O_2]$ $((2.10\pm0.55).10^{-2}$ with a coefficient of variation of 26%).

Table S2: Data for Figure 1 (sequential triple injection of DTT) for both linear and quadratic dependence on $[O_2]$.

Initial slope of O_2 Consumption [μmol min^{-1}]	O_2 concentration at time of DTT addition	Initial rate constant using $[O_2]^1$ in rate expression	Initial rate constant using $[O_2]^2$ in rate expression
0.102	3.80 (at 34 minutes)	0.0268	$7.06.10^{-3}$
0.0546	2.68 (at 68 min.)	0.0204	$7.60.10^{-3}$
0.0284	1.79 (at 104 min.)	0.0159	$8.86.10^{-3}$

Quantification of quinones in the SRM 2975 diesel particle

As quinones are reported to be correlated to the DTT redox activity,[2, 3] we used a slightly modified analytical method described by Cho et al.[4] for the determination of the 1,2-naphtoquinone (1,2-NQ), 1,4-naphtoquinone (1,4-NP), 9,10-anthraquinone (9,10-AQ) and the 9,10-phenanthraquinone (9,10-PQ). Toluene instead of dichloromethane was used for the extraction of the quinones and 9,10-anthraquinone-d_8 was used as internal standard. After acetylation of the carbonyl functional group with acetic anhydride and metallic zinc, the derivative was extracted with pentane. The organic extract was concentrated to dryness and reconstituted in toluene. The analytes were quantified by injecting the sample in a GC-MS instrument. Table S3 presents the mass concentrations of these four quinones in the SRM 2975 reference material as well as the analytical figure of merit.

Table S3: Quinones concentrations in the SRM 2975 reference material (toluene extract) as well as the analytical limits of detection, quantification and recovery. The number of repetition is indicated in bracket.

	1,2-NQ	1,4-NQ	9,10-AQ	9,10-PQ
SRM 2975 concentration [μg g^{-1}]	3.9 ± 1.5 (17)	< LOD	11.9 ± 2.6 (26)	12.5 ± 1.9 (22)
Limit of detection [μg g^{-1}]	1.2	1.5	1.5	2.0
Limit of quantification [μg g^{-1}]	3.6	4.5	4.5	6.0
Recovery [%]	104 ± 26 (18)	94 ± 24 (18)	100 ± 14 (18)	91 ± 34 (18)

Surface characteristics by FTIR

Infrared spectral data are used to study the functional group on the surface of the studied particles. The assignment of vibrational bands of specific functional groups presented in Figure S5 was carried out in comparison with published work.[5-7] The main characteristics of the FTIR spectra presented for all three samples are the broad peak centered at 3440 cm^{-1}, a peak at 1600-1630 cm^{-1} and a broad band between1150-1270 cm^{-1}. In addition, FW2 and SRM 2975 present a distinct peak at 1720-1740 cm^{-1}. The 3440 cm^{-1} band is assigned to the (O-H) stretching vibration of a carboxylic group, adsorbed water or OH stretch frequency of an aromatic alcohol such as a hydroquinone. The peak observed for the three NP's in the range 1630 to 1740 cm^{-1} is naturally attributed to the carbonyl stretch frequency and/or the conjugated double bond of a quinone-like structure.[5,7-9] According to Coates,[7] quinones or conjugated ketones have a carbonyl stretch vibration absorbing at both 1675-1690 cm^{-1} with a 1600-1650 cm^{-1} band belonging to the conjugated C=C double bond stretch vibration whereas isolated carbonyl groups absorb at 1705-1725 cm^{-1}. The 1720 and 1740 cm^{-1} absorption in SRM 2975 and FW2 are attributed to carbonyl stretch vibrations because the carbonyl absorption frequency increases with increasing numbers

of fused rings.[7] In agreement with the data on NH_2OH uptake displayed in Table S1 the abundance of carbonyl sites is at least a factor of 120 and 8.0 smaller for Printex 90 compared to SRM 2975 and FW2, respectively, when considering the surface density of carbonyl sites for SRM 2975, FW2 and Printex 90, respectively ($1.4\ 10^{15}$, $9.6\ 10^{13}$, $1.2\ 10^{13}$ molecule cm^{-2}). The quantitative surface data suggest that the carbonyl stretch frequency disappeared in the noise level in the case of Printex 90. For this last particle, the carbonyl absorption is weaker and the distinct 1630 cm^{-1} band is associated with the conjugated C=C double bonds interacting with the C=O bond.[10] The carbonyl stretch vibration of the carboxylic group absorbs in the range 1700-1725 cm^{-1} but is deemed less important in this case owing to the smaller number of carboxylic groups compared to carbonyl groups (Table S1). The broad band in the 1300-1000 cm^{-1} region corresponds to a combination of C-C, C-H in-plane deformation as well as ether C-O-C stretching groups. These experimental data are consistent with the expected properties of compounds such as quinones that have redox-cycling capabilities as they display the mid-IR signature of the expected functional groups. However, quantitation on the sole basis of FTIR absorption spectroscopy does not seem possible owing to the complex composition of the soot samples.

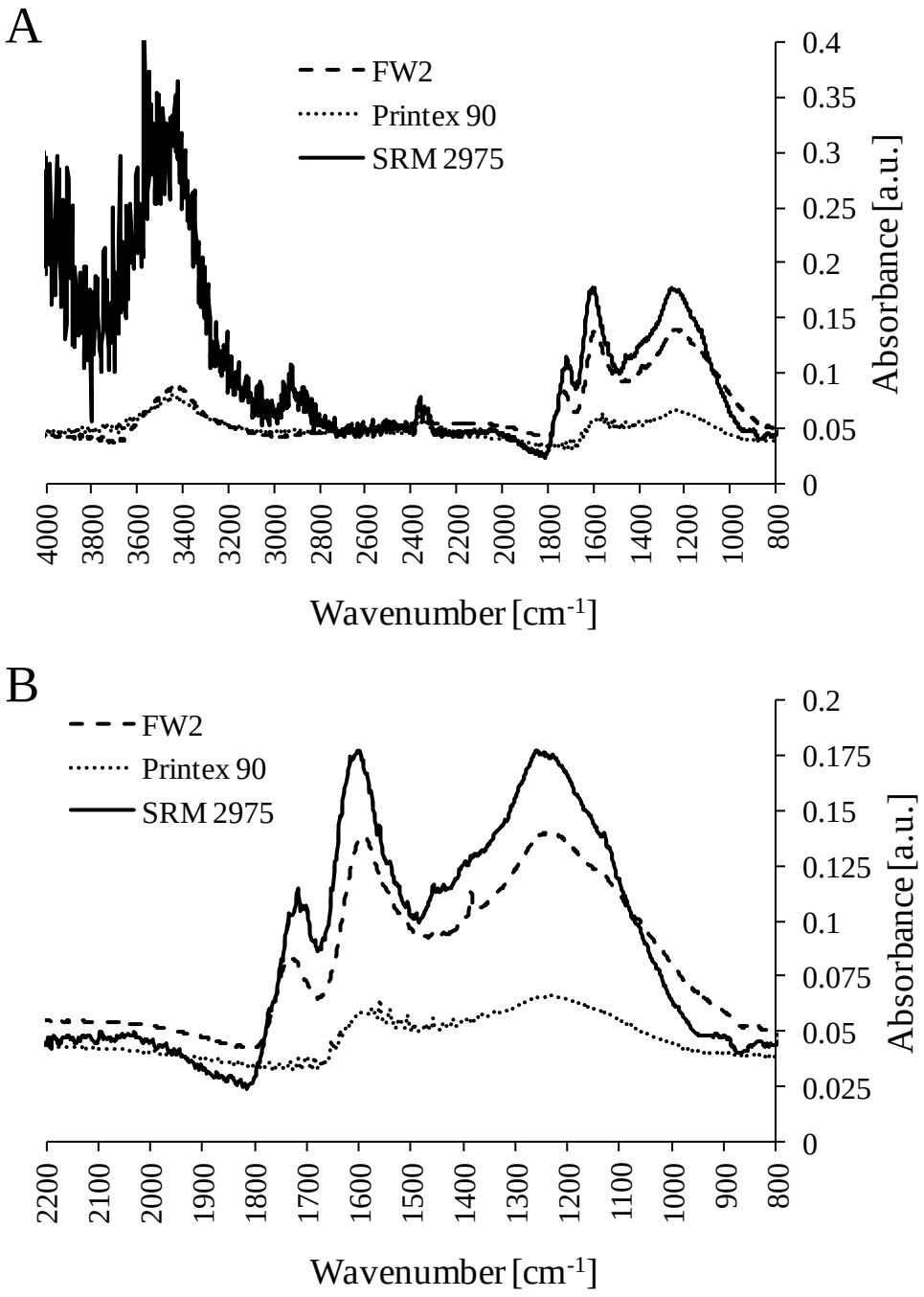

Figure S5: FTIR of the three different NP materials studied in this work. The mass ratio between the particle and the KBr was 0.05%, 0.03% and 0.16% for FW2, Printex 90 and SRM 2975 respectively. **A.** Absorbance for the wavenumber range from 800 – 4000 cm^{-1}. **B.** Enlargement of the FTIR part for wavenumber in the range 800-2200 cm^{-1}.

References

(1) Sauvain, J.-J.; Rossi, M. J.; Riediker, M. Comparison of Three Acellular Tests for Assessing the Oxidation Potential of Nanomaterials. *Aerosol Sci. Technol.* **2013**, 47, (2) 218-227.

(2) Kumagai, Y.; Koide, S.; Taguchi, K.; Endo, A.; Nakai, Y.; Yoshikawa, T.; Shimojo, N. Oxidation of proximal protein sulfhydryls by phenanthraquinone, a component of diesel exhaust particles. *Chem. Res. Toxicol.* **2002**, 15 (4), 483-489.

(3) Ntziachristos, L.; Froines, J. R.; Cho, A. K.; Sioutas, C. Relationship between redox activity and chemical speciation of size-fractionated particulate matter. *Part. Fibre Toxicol.* **2007**, 4, 5; DOI 10.1186/1743-8977-4-5.

(4) Cho, A. K.; Di Stefano, E.; You, Y.; Rodriguez, C. E.; Schmitz, D. A.; Kumagai, Y.; Miguel, A. H.; Eiguren-Fernandez, A.; Kobayashi, T.; Avol, E.; Froines, J. R. Determination of four quinones in diesel exhaust particles, SRM 1649a, an atmospheric PM2.5. *Aerosol Sci. Technol.* **2004**, 38, 68-81.

(5) Sutherland, I.; Sheng, E.; Bradley, R. H.; Freakley, P. K. Effects of ozone oxidation on carbon black surfaces. *J. Mater. Sci.* **1996**, 31 (21), 5651-5655.

(6) Holder, A. L.; Carter, B. J.; Goth-Goldstein, R.; Lucas, D.; Koshland, C. P. Increased cytotoxicity of oxidized flame soot. *Atmos. Pollut. Res.* **2012**, 3 (1), 25-31.

(7) Coates, J. Interpretation of Infrared Spectra, A Practical Approach. In *Encyclopedia of Analytical Chemistry*; Meyers, R. A., Eds.; Chichester, 2000; pp 10815–10837.

(8) Antinolo, M.; Willis, M. D.; Zhou, S.; Abbatt, J. P. D. Connecting the oxidation of soot to its redox cycling abilities. *Nature Communications* **2015**, 6; DOI 10.1038/ncomms7812.

(9) Jager, C.; Henning, T.; Schlögl, R.; Spillecke, O. Spectral properties of carbon black. *J. Non Cryst. Solids* **1999**, 258 (1-3), 161-179.

(10) Peebles, B. C.; Dutta, P. K.; Waldman, W. J.; Villamena, F. A.; Nash, K.; Severance, M.; Nagy, A. Physicochemical and Toxicological Properties of Commercial Carbon Blacks Modified by Reaction with Ozone. *Environ. Sci. Technol.* **2011**, 45 (24), 10668-10675.